

# Comprehensive characterization of human bone marrow microenvironment shows age-related changes

The bone marrow microenvironment (BME) is vital for controlling hematopoietic output. Qualitative and quantitative changes in the BME contribute to perturbations of hematopoiesis during physiological stress, aging, and hematological malignancies. Murine models primarily inform the current knowledge of the BME and its functional implications for hematopoiesis. Using such models, it has become evident that during aging, the bone marrow experiences high levels of interleukin (IL)1 $\beta$ , TNF $\alpha$ , and C-reactive protein and thus, a chronic low-grade inflammatory environment.<sup>1</sup> Murine models of myeloproliferative neoplasm have linked the overproduction of IL1 $\beta$  to disruptions in the mesenchymal stroma cell (MSC) populations in the bone marrow and downregulation of CXCL12<sup>2</sup> illustrating the potential of inflammation to induce changes in hematopoietic stem and progenitor cells (HSPC) via dysregulation of the BME. The use of genetically engineered mouse models combined with cell sorting and transcription factor lineage tracing led to the characterization of specialized niches in the mouse bone marrow.<sup>1,3,4</sup> Whereas single-cell RNA sequencing and spatial transcriptomics helped create a detailed atlas of the murine BME,<sup>5,6</sup> less is known about the human BME. In efforts to characterize the human BME, emerging single-cell RNA sequencing studies,<sup>6,7</sup> combined with protein-based imaging<sup>8</sup> have investigated human BME under both steady-state and disease conditions, examining various immunophenotypically defined BME subsets.<sup>9</sup> Considerable overlap between murine and human BME appears to exist. For instance, MSC from older individuals have lower expression of CXCL12<sup>10</sup> and an altered cytokine profile that might be linked to aging-associated changes in hematopoiesis: expansion of the HSPC compartment, myeloid bias, immune senescence, and anemia.<sup>11</sup> While CD271<sup>+</sup> MSC are an important component of the bone marrow, a comprehensive atlas of the human BME is currently actively being constructed. A major limitation is that non-hematopoietic cells constitute less than 1-2% of the human BME.<sup>12</sup> To address this challenge, we employed minimal enrichment and negative selections to enhance cell recovery and ensure appropriate diversity of cellular BME populations. To this end, we used bone marrow aspirates from young individuals selected as healthy donors for allogeneic bone marrow transplantation at Johns Hopkins University between 2020 and 2021. The study was performed under a research protocol approved by the Johns Hopkins Institutional Review Board and patients consented under the Declaration of Helsinki. Data were generated from eight individuals, with a median of 3,409 cells (interquartile range [IQR], 1,019-5,150) per donor

(*Online Supplementary Table S1*). Bone marrow samples were digested with collagenase and DNase I, and CD45<sup>+</sup> cells were depleted using Rosettesep antibody cocktail. We further used cell sorting to enrich for alive (7AAD<sup>-</sup>), nucleated (Vybrant DyeCycle<sup>+</sup>) cells lacking expression of hematopoietic (CD45), erythroid (CD235a, CD71), and plasma cell (SLAMF7) markers (*Online Supplementary Figure S1*). Subsequently cells underwent single-cell RNA sequencing using 10xGenomics platform and 3'-end capture. We identified five distinct populations: MSC, osteolineage cells (OLC), smooth muscle cells (SMC), fibroblasts, and endothelial cells (EC) (Figure 1A). Notably, adipocytes which were not identified here, may be better captured by single-nucleus RNA sequencing. Given the extensively characterized murine BME atlas, we used publicly available murine scRNAseq datasets<sup>6</sup> to create a "humanized" mouse matrix by converting mouse genes to their human orthologs, refining human BME clusters and evaluating their overlap with known mouse BME populations (*Online Supplementary Figure S2A*).

MSC constituted the predominant population in human BME, comprising more than 90% of the total cells captured. MSC were characterized by high expression of CXCL12, LEPR (Figure 1B) and PDGFRA, a marker previously reported in murine and human Nestin-positive cells (*Online Supplementary Figure S2B*). The cluster was enriched for genes suggestive of trilineage differentiation programs: adipocyte (LPL, APOE, ANGPTL4), osteogenic (RUNX1, ALPL, CDH11), and chondrocyte differentiation (SOX9). Additionally, gene expression suggested the hematopoietic support function of MSC through the expression of CXCL12, KITLG, and ANGPT1 (*Online Supplementary Figure S2B*).

Detailed analysis of the MSC clusters revealed the presence of a subpopulation (MSC1) with an inflammatory signature. Genes implicated in mediating inflammation, such as the chemokine-encoding CXCL2 and CCL2, inflammation-induced transcription factor CEBPB, and TNF- $\alpha$ -inducible regulator TNFAIP3 were among the most differentially expressed genes in the MSC1 subpopulation. AP-1 complex genes (FOSB, JUND) also showed upregulated expression in the MSC1 cluster. On the other hand, the transcriptomic profile of MSC2 suggests the presence of adipo-primed progenitor cells, supported by the upregulation of LPL and APOE. Comparison between murine and human BME maps showed extensive overlap of MSC1 and MSC2 with the fibroblastic reticular-niche-lepr-stromal population (50-90%, >90% respectively), suggesting the existence of a human correlate of murine CXCL12-rich abundant reticular cells (Figure 1C). Notably, in our analysis, CD271

(*NGFR*) transcripts are present in the MSC but absent in EC and SMC clusters. Thus, the current strategy better captures the diversity of the human BME compared to methods using CD271 selection. The OLC cluster included osteoblasts at various stages of differentiation, from immature (*SP7/OSX*, *SPP1*, *IBSP*) to maturing and mature osteoblasts (*BGLAP*), offering the opportunity to study the interaction of distinct osteolineage clusters with HSPC populations. As suggested by murine studies, differential production of *SPP1* by OLC may impact HSC quiescence and retention.<sup>13</sup> The OLC transcriptome also aligned with murine osteoblast profiles (Figure 1C). The SMC cluster, defined by high expression of *MYH11*, *ACTA2* and *RGS5* (Figure 1B), is transcriptomically similar to the murine Stroma-Myh11-high cells (Figure 1C). These cells, particularly the SMC2 subcluster express moderate levels of *CXCL12* and high levels of *CD146* (MCAM) and *LMOD1* (Online Supplementary Figure S2B) and were recently similarly annotated as vascular smooth muscle cells in humans.<sup>8</sup> The fibroblast population was identified by expression of *S100A4*, *S100A6*, and *S100A10* (Figure 1B). Receptor-ligand analysis suggests a strong interaction

between fibroblast-produced *DPP4* (a *CXCL12* peptidase) and *CXCL12* produced by MSC1 and MSC2 clusters (Online Supplementary Figure S2C). Thus, fibroblasts may indirectly regulate hematopoiesis by modulating *CXCL12* availability. In addition, these cells play an essential role in generating the bone marrow matrix as suggested by high expression of collagen-type encoding genes (*COL1A1*, *COL6A1/2*, *COL15A1*, *COL12A1*), a role akin to the murine col23<sup>+</sup>Stromal-Il33-high population with which they share moderate transcriptional overlap (Figure 1C). The EC cluster was defined by expression of *PECAM1*, *SELE*, and *CDH5* (Figure 1B) as well as *CD34*, *THBD*, *CLDN5*, and *FLT1* (Online Supplementary Figure S2B), with transcriptomic similarity to murine Niche-vecad-Endothelial-Arterial-Cd34-high cells (Figure 1C). To evaluate whether our approach detects subtle molecular changes proposed to be associated with BME aging, we compared our (JHU) cohort to healthy samples from de Jong *et al.* (de Jong cohort)<sup>12</sup> (Online Supplementary Table S1). We identified similar cell clusters in the de Jong cohort, including MSC1, MSC2, OLC and EC populations (Figure 2A, B), and largely maintained their correlation with

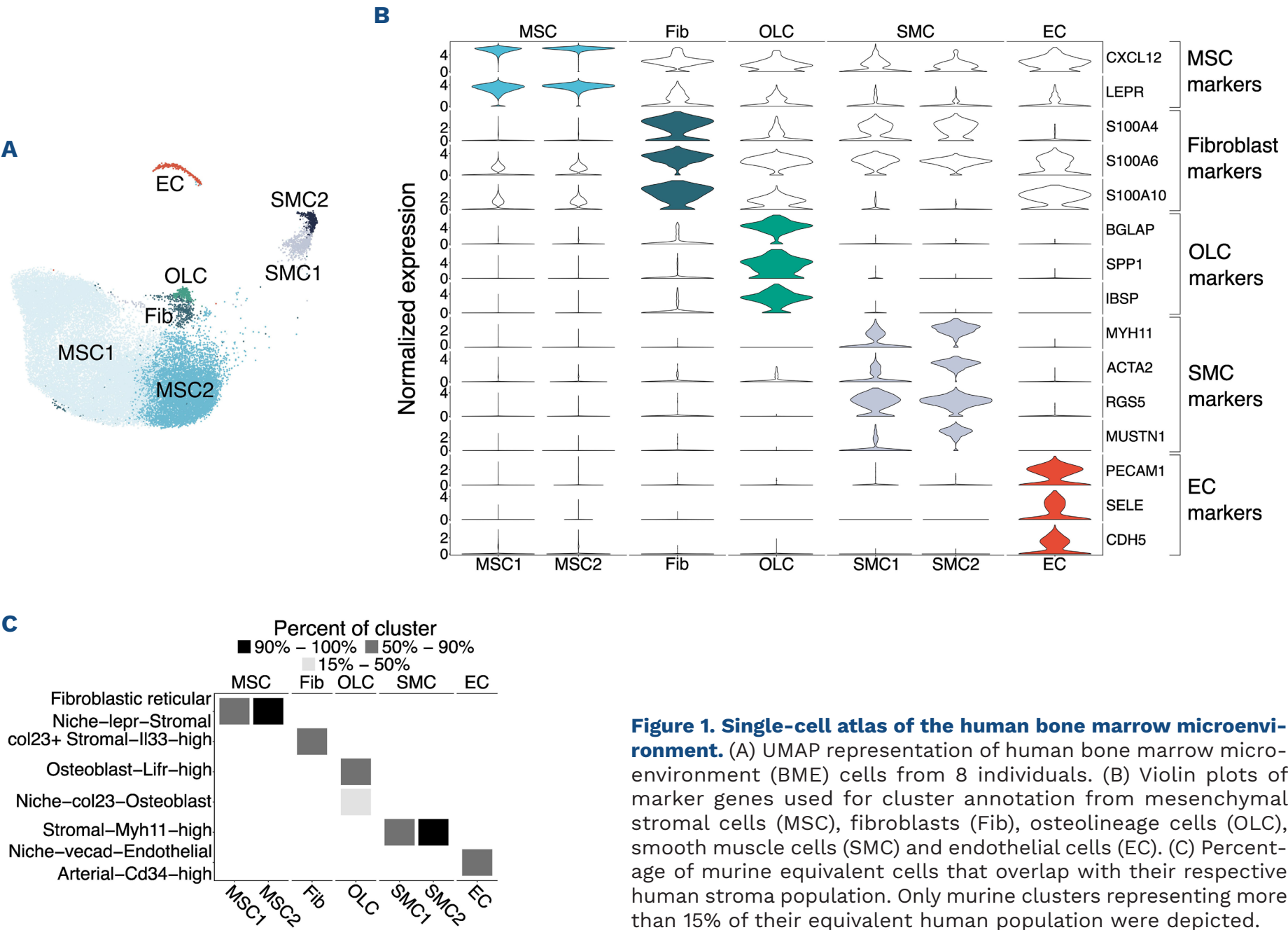


**Figure 1. Single-cell atlas of the human bone marrow microenvironment.** (A) UMAP representation of human bone marrow microenvironment (BME) cells from 8 individuals. (B) Violin plots of marker genes used for cluster annotation from mesenchymal stromal cells (MSC), fibroblasts (Fib), osteolineage cells (OLC), smooth muscle cells (SMC) and endothelial cells (EC). (C) Percent of murine equivalent cells that overlap with their respective human stroma population. Only murine clusters representing more than 15% of their equivalent human population were depicted.

the murine BME populations (*Online Supplementary Figure S2D*). Some quantitative differences can be seen between the two data sets, particularly the presence of an additional fibroblast cluster in the JHU cohort. It is tempting to speculate that these differences are age-related, though there are significant technical discrepancies between the two methods to account for these results. Thus, we have focused our analysis on qualitative differences between the two datasets. Interestingly, de Jong samples appear to have lower *CXCL12* and *LEPR* expression levels in the MSC1 population (*Figure 2B*). Since the de Jong cohort is skewed toward patients of older age (range, 72–75 years) (*Online Supplementary Table S1*), we tested if qualitative differences may be secondary to transcriptomic changes in the BME cells isolated from old and young individuals. The MSC1 cluster transcriptomes revealed upregulation of AP-1 complex genes (*JUN*, *JUND*, *JUNB*, *FOS*) in old compared to young individuals, suggesting a potential dominance of the pro-inflammatory cluster in the aged BME (*Online Supplementary Figure S2E*). Interestingly,

we observed downregulation of *CXCL12* (*Figure 2C*) and *KITLG* (*Figure 2D*) in the same populations. Thus, similar to murine models, a pro-inflammatory environment in the bone marrow might lead to the downregulation of *CXCL12* expression in older individuals. The impact on *CXCL12* availability may be further augmented by dysregulated post-translational modifications and increased protein degradation of *CXCL12*. To this end, even though our method captures a significant population of fibroblasts that could modulate *CXCL12* availability via *DPP4* (*Online Supplementary Figure S2C*), the published datasets available from older individuals do not contain sufficient numbers of these cells to assess if *DPP4* levels are affected by aging. It is evident, however, that aging alters BME structure, as suggested by decreased expression of extracellular matrix mRNA transcript such as *CDH11*, *TNC*, and *VCAN*, as well as *COL14A1*. The method presented here serves as a stepping stone toward comprehensive qualitative and quantitative assessment of the aging BME, although further validation is needed to

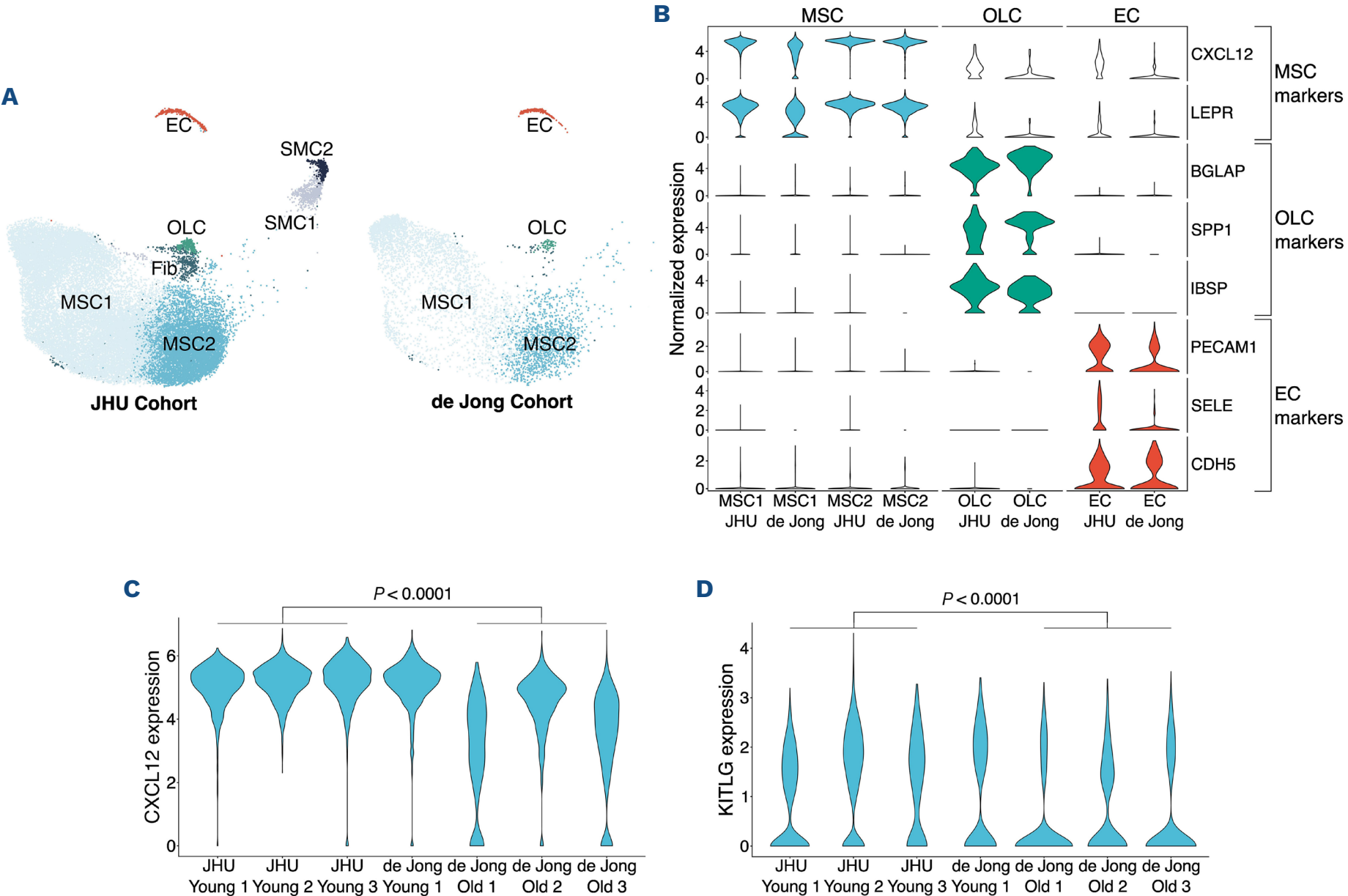


**Figure 2. Comparison of old and young human bone marrow microenvironment.** (A) UMAP representation of human bone marrow microenvironment (BME) cells from the current dataset (JHU cohort) and previously published reports (de Jong cohort). (B) Violin plots of marker genes used for cluster annotation between the JHU and de Jong datasets from mesenchymal stromal cells (MSC), fibroblasts (Fib), osteolineage cells (OLC), smooth muscle cells (SMC) and endothelial cells (EC). Violin plots depicting (C) *CXCL12* and (D) *KITLG* expression in the MSC1 population between old versus young subjects.  $P$  values were computed using Wilcoxon Rank Sum test.



account for discrepancies between the two methods, ensuring that observed changes reflect true biological differences rather than methodological variation. While the JHU and de Jong cohort comparison captures some aging-related molecular changes of the BME, it is essential to highlight that the older “healthy” samples came from patients with cardiovascular disease requiring cardiac surgery or advanced arthritis requiring hip arthroplasty, a population with a very high (~40%) incidence of clonal hematopoiesis (CH).<sup>14,15</sup> Considering the suggested correlation between CH and chronic inflammation, it would be valuable to determine how much of the observed transcriptomic differences are specifically associated with CH.

## Authors

Mareike Peters,<sup>1\*</sup> Patric Teodorescu,<sup>1\*</sup> Sergiu Pasca,<sup>1</sup> Xuan Zhang,<sup>2</sup> Rulin Wang,<sup>1</sup> Srinivasan Yegnasubramanian,<sup>1</sup> H. Leighton Grimes,<sup>2,3,4</sup> Nathan Salomonis,<sup>3,5</sup> Lukasz P. Gondek<sup>1</sup> and Gabriel Ghiur<sup>1</sup>

<sup>1</sup>Sidney Kimmel Comprehensive Cancer Center, Johns Hopkins University School of Medicine, Baltimore, MD; <sup>2</sup>Division of Immunobiology, Cincinnati Children’s Hospital Medical Center, Cincinnati, OH; <sup>3</sup>Department of Pediatrics, University of Cincinnati, Cincinnati, OH; <sup>4</sup>Division of Experimental Hematology and Cancer Biology, Cincinnati Children’s Hospital Medical Center, Cincinnati, OH and <sup>5</sup>Division of Biomedical Informatics, Cincinnati Children’s Hospital Medical Center, Cincinnati, OH, USA

*\*MP and PT contributed equally as first authors.*

Correspondence:

G. GHIAR – gghiaur1@jhmi.edu

## References

- Pioli PD, Casero D, Montecino-Rodriguez E, Morrison SL, Dorshkind K. Plasma cells are obligate effectors of enhanced myelopoiesis in aging bone marrow. *Immunity*. 2019;51(2):351–366.e6.
- Arranz L, Sánchez-Aguilera A, Martín-Pérez D, et al. Neuropathy of haematopoietic stem cell niche is essential for myeloproliferative neoplasms. *Nature*. 2014;512(7512):78–81.
- Pinho S, Frenette PS. Haematopoietic stem cell activity and interactions with the niche. *Nat Rev Mol Cell Biol*. 2019;20(5):303–320.
- Pisterzi P, Chen L, van Dijk C, Wevers MJW, Bindels EJM, Raaijmakers MHGP. resource: a cellular developmental taxonomy of the bone marrow mesenchymal stem cell population in mice. *Hemasphere*. 2023;7(2):e823.
- Tilburg J, Stone AP, Billingsley JM, et al. Spatial transcriptomics of murine bone marrow megakaryocytes at single-cell resolution. *Res Pract Thromb Haemost*. 2023;7(4):100158.
- Baryawno N, Przybylski D, Kowalczyk MS, et al. A cellular taxonomy of the bone marrow stroma in homeostasis and leukemia. *Cell*. 2019;177(7):1915–1932.e16.
- Chen L, Pronk E, Van Dijk C, Bian Y, Feyen J, Van Tienhoven T, et al. A single-cell taxonomy predicts inflammatory niche remodeling to drive tissue failure and outcome in human AML. *Blood Cancer Discov*. 2023;4(5):394–417.
- Bandyopadhyay S, Duffy MP, Ahn KJ, Sussman JH, Pang M, Smith D, et al. Mapping the cellular biogeography of human bone marrow niches using single-cell transcriptomics and proteomic imaging. *Cell*. 2024;187(12):3120–3140.e29.
- Li H, Bräunig S, Dhapolar P, Karlsson G, Lang S, Scheduling S. Identification of phenotypically, functionally, and anatomically distinct stromal niche populations in human bone marrow based on single-cell RNA sequencing. *Elife*. 2023;12:e81656.
- Periyasamy-Thandavan S, Burke J, et al. MicroRNA-141-3p negatively modulates SDF-1 expression in age-dependent pathophysiology of human and murine bone marrow stromal cells. *J Gerontol A Biol Sci Med Sci*. 2019;74(9):1368–1374.
- Geiger H, de Haan G, Florian MC. The ageing haematopoietic stem cell compartment. *Nat Rev Immunol*. 2013;13(5):376–389.
- de Jong MME, Kellermayer Z, Papazian N, et al. The multiple

<https://doi.org/10.3324/haematol.2025.287536>

Received: March 3, 2025.

Accepted: May 23, 2025.

Early view: June 5, 2025.

©2025 Ferrata Storti Foundation

Published under a CC BY-NC license 

### Disclosures

GG received research funding from Abbvie Inc., Menarini Recherche, Kinomica Inc. and Arcellx Inc. GG served on the advisory board of Syros Inc.

### Contributions

MP wrote the manuscript and analyzed data. PT wrote the manuscript and performed research. SP analyzed sequencing data. XZ and RW contributed to setting up the original scRNAseq experiments. SY, HLG, NS and LPG analyzed the data. GG designed and coordinated the project. All authors critically reviewed the manuscript.

### Funding

MP, PT, SG, LPG, GG were supported by Break Through Cancer. WZ, HLG, NS, GG are supported by R01 CA253981. RW, SY, GG are supported by P30 CA006973. GG is supported by P01 CA225618.

### Data-sharing statement

The data that support the findings of this study have been deposited in Zenodo and are publicly available at <https://doi.org/10.5281/zenodo.15283660> (DOI 10.5281/zenodo.15283660). Any additional data is available from the corresponding author upon request.

- myeloma microenvironment is defined by an inflammatory stromal cell landscape. *Nat Immunol.* 2021;22(6):769-780.
13. Stier S, Ko Y, Forkert R, et al. Osteopontin is a hematopoietic stem cell niche component that negatively regulates stem cell pool size. *J Exp Med.* 2005;201(11):1781-1791.
14. Hecker JS, Hartmann L, Rivière J, et al. CHIP and hips: clonal hematopoiesis is common in patients undergoing hip arthroplasty and is associated with autoimmune disease. *Blood.* 2021;138(18):1727-1732.
15. Jaiswal S, Natarajan P, Silver AJ, et al. Clonal hematopoiesis and risk of atherosclerotic cardiovascular disease. *N Engl J Med.* 2017;377(2):111-121.